Conf-8210116--2

SOLUTION HARDENING AND STRAIN HARDENING AT ELEVATED TEMPERATURES*

U. F. Kocks
Materials Science & Technology Division
Argonne National Laboratory
Argonne, IL 60439

CONF-8210116--2

DE83 007745

OCTOBER 1982

DISCLAIMER

---

*Work supported by the U. S. Department of Energy.
Work is being submitted to the 1982 ASM Materials Science Seminar "Deformation, Processing, and Structure, sponsored by the American Society for Metals, October 23-24, 1982, Sheraton St. Louis, St. Louis, Missouri.
(INVITED TALK)

SOLUTION HARDENING AND STRAIN HARDENING AT ELEVATED TEMPERATURES

U. F. Kocks

Materials Science and Technology, Argonne National Laboratory, Argonne, IL 60439

Abstract

Solutes can significantly increase the rate of strain hardening; as a consequence, the saturation stress, at which strain hardening tends to cease for a given temperature and strain rate, is increased more than the yield stress: this is the major effect of solutes on strength at elevated temperatures, especially in the regime where dynamic strain-aging occurs. It is shown that local solute mobility can affect both the rate of dynamic recovery and the dislocation/dislocation interaction strength. The latter effect leads to multiplicative solution strengthening. It is explained by a new model based on repeated dislocation unlocking, in a high-temperature limit, which also rationalizes the stress dependence of static and dynamic strain-aging, and may help explain the "plateau" of the yield stress at elevated temperatures.

1. INTRODUCTION

Neither solution hardening nor strain hardening occupy a prominent place in most discussions of high-temperature strength. This article is an attempt to show that they are, in fact, important phenomena, particularly in the many instances when they reinforce each other. In the regime of dynamic strain-aging, both the importance of solutes and their effect on strain hardening have been realized for a long time; but we shall demonstrate that this synergism holds much more generally.

When "strength" is discussed at elevated temperatures, the concern is not so much with yield as with the flow stress at large strains (for applications to forming processes) or (for structural applications) with the "creep strength". Both relate to a regime of the stress strain curve in which the rate of strain hardening is low, approaching steady-state flow. However, the stress level at which this steady-state limit is reached is itself a property of strain hardening: it is controlled by a dynamic balance between hardening and (dynamic) recovery mechanisms (Sec.2). Thus, any metallurgical change that affects strain hardening affects the elevated-temperature strength.

The principal effect of solution hardening that is usually considered is an additive friction stress [1-3] (Sec.3). Such a friction stress adds to the steady-state stress just as it adds to the yield stress. Inasmuch as this friction stress decreases rapidly with temperature, however, it should not affect the high-temperature strength very much: even though the yield stress usually reaches a "plateau" at elevated temperatures, it is small compared to the stress increment due to strain-hardening.

When solutes are mobile, they appear not only to decrease the mobility of mobile dislocations (thus increasing the friction stress), but also to slow down the rate of rearrangement of stored dislocations (thus decreasing dynamic

recovery and increasing strain hardening) [4-6] (Sec.4). The latter effect can, in addition, be caused by a decrease in the stacking-fault energy due to the solute addition [1] (Sec.5). For both reasons, the flow stress at large strains can be significantly increased by solution hardening, even when the yield stress is not.

Finally, there are a number of cases in which the effect of solutes on strain hardening appears to be multiplicative: the rate of strain hardening and the flow stress, throughout the stress strain curve, are multiplied by the same, concentration-dependent factor (Sec. 6). In mechanistic terms, this observation may be expressed as an increase in the effectiveness of forest hardening by the solutes [7].

A unifying mechanism is proposed that relates multiplicative solution hardening to recent observations in static and dynamic strain-aging [8,9]. It is based on a dislocation unlocking model, which has been successful in explaining many aspects of low-temperature solution hardening [10,11]. The new feature is the high-temperature limit. It arises because the length of the activation bulge, which increases with temperature, cannot exceed the forest dislocation spacing: from that point on, the solutes effectively increase the dislocation/forest interaction strength (Sec. 7).

In summary, strain hardening can be severely influenced by solute elements in two distinct ways: one relates to a change in the evolution of the substructure, the other to the effectiveness of a given structure. Both lead to significant effects on the near-steady-state strength at elevated temperatures. Procedures are proposed for separating the different effects experimentally (Sec.8).

In this article, we shall not discuss effects at either very small or very large strains: yield drops and Lüders front propagation were recently

dealt with by the author[12], and effects of solutes on the tensile strength after wire drawing or rolling have also been recently discussed in the literature [2,13,14]. In the mechanistic discussions, we will ignore potential effects of small precipitates or ordered regions in nominal "solid solution"; these have also been amply discussed [5,2,6].

2. STRAIN HARDENING AND HIGH-TEMPERATURE STRENGTH

Figure 1 shows a set of stress strain curves as a function of temperature that is typical at least for pure fcc materials, both as polycrystals and as single crystals in multiple-slip orientations [15-18]. A noteworthy feature of these curves is that they coincide for small strains. This observation, together with more detailed considerations, have led Mecking and Kocks[18] to identify an initial "athermal hardening" component Θ_h of the strain-hardening rate $\Theta = d\sigma/d\varepsilon$ (much as a "Stage II" of hardening had been identified previously in single crystals[19]). The remaining component is then defined as the rate of dynamic recovery, Θ_r:

$$\Theta = \Theta_h - \Theta_r(\sigma,T,\dot{\varepsilon}) \qquad (1)$$

As is indicated in eq.(1), all the dependence on stress, temperature, and strain rate is associated with the dynamic-recovery term. (A slight stress dependence of Θ_h is not ruled out, but is assumed negligible with respect to that of Θ_r.) In fact, the athermal hardening rate is insensitive even to material, being, in tension, of the order of 1/50 of Young's modulus.

The strain-hardening rate decreases continuously; in fact it decreases rapidly enough that, by one extrapolation method or another, a limit may be defined where it would vanish[20,17,21]. We shall here not be concerned with whether this steady-state limit is actually reached[22]: we will use it merely as a semi-quantitative indication of the flow stress when strain hardening is

low. This "saturation stress" and its dependence on temperature and strain rate then follow from a solution of eq.(1) for $\Theta = 0$.

Figure 2 illustrates the temperature dependence of the saturation stress for aluminum polycrystals, as determined from a (short) extrapolation of the curves in Fig. 1 [17]. The saturation stress decreases roughly exponentially with temperature (the plot of its logarithm being roughly linear in temperature) and does so much more strongly than the yield stress.* Despite this rapid decrease, the absolute value of the saturation stress is still significant at two-thirds of the melting temperature (the last point in Fig. 2): it is still about six times the yield stress.

The point that will be made for solution hardened alloys is that the steady-state stress vs temperature line is more significantly influenced by solute additions than the yield stress line; thus, the "strength", especially as it relates to elevated-temperature applications, can be more efficiently increased through an effect on strain hardening than on the friction stress.

3. ADDITIVE SOLUTION HARDENING

The flow stress of solid solutions is usually described by an expression of the form [1-3]

$$\sigma = \sigma_f + \sigma_d \qquad (2)$$

Here, σ_f indicates a "friction stress" due to the interaction of solutes with mobile dislocations; it is strongly temperature and rate dependent. The second term, σ_d, is due to dislocation/dislocation interactions and generally of the form

$$\sigma_d = M \alpha \mu b \sqrt{\rho} \qquad (3)$$

---

* The yield stresses were evaluated from the same data that were partially reported in [15].

where M is the Taylor factor converting crystallographically resolved shear stresses (glide resistances) into the relevant stress component in the macroscopic coordinates, μ is the shear modulus, b the magnitude of the Burgers vector, and ρ the dislocation density; α is a proportionality factor a little less than 1, which is also meant to reflect the slight temperature and strain-rate dependence of dislocation cutting [18].

Equation (2) neglects other contributions to the flow stress that may, in certain applications, be significant; e.g., due to the grain size. We shall assume here, however, that none of these other processes produces significant strain hardening. (For this reason, we must specifically exclude second-phase particles.) Then, we can write (from eqs. 2 and 3)*

$$\Theta \equiv \frac{\partial \sigma}{\partial \varepsilon}\Big|_{T,\dot{\varepsilon}} = M^2 \alpha \mu b \frac{d\sqrt{\rho}}{d\gamma} \qquad (4)$$

The important physical process that controls strain hardening is the rate of dislocation accumulation with the glide increment $d\gamma = M\, d\varepsilon$; its two components, statistical storage and dynamic recovery, give rise to the two components of Θ (eq. 1).

The essence of eqs.(2) and (4) is that the classical solute friction stress does not contribute to strain hardening: the stress strain curves should merely be shifted upward. Figures 3 to 5 show the best cases I could find that approximately obey this rule; all relate to deformation at low temperature (77 K) and to rather small strains [23-25].

In these cases, if the behavior can be properly extrapolated to large strains, the steady-state stress would be augmented by exactly the same amount as the yield stress. At elevated temperatures, this would be proportionately very little. In the following, we will discuss cases where solutes are

---

* Any influence of a strain dependence of the mobile dislocation density (or of the vacancy concentration) on σ_f in eq. (2) have been neglected.

observed to influence strain hardening as well as the yield stress. This is possible, according to eq.(4), if solutes can affect either the rate of dislocation accumulation $d\sqrt{\rho}/d\gamma$ or the proportionality constant α. Both effects will be shown to exist. (In addition, of course, there is the trivial effect of solutes on the shear modulus and the Burgers vector.)

4. DYNAMIC STRAIN-AGING AND DYNAMIC RECOVERY

Figure 6 shows the case of an especially strong influence of solute concentration on stress strain behavior in Ni-C [9]. Note, however, that the curves diverge much more strongly at large strains than at small. In first approximation one can say that the predominant effect of solutes is here to decrease Θ_r.

These stress strain curves were taken in the regime where jerky flow (the Portevin-LeChatelier effect) is observed.* It appears, then, that dynamic strain-aging affects not only the mobility of the mobile dislocations (and thus the character of flow), but also the ease of rearrangement of the previously stored dislocations (and thus dynamic recovery) [4,5]. Further evidence for this interpretation is that the rate sensitivity of strain hardening is negative in the dynamic-recovery regime, not only the rate sensitivity of the flow stress (Fig. 6).

It has, in fact, long been known that the "hump" in flow stress vs temperature diagrams in the dynamic strain-aging regime is more pronounced for the ultimate tensile strength than for the yield strength; e.g., in Fe-N [26] and Type 316 Stainless Steel [27]. Figures 7 and 8 show this feature for Hadfield steel [28] and for INCONEL 600 [29]. (In the latter, the extrapolated

---

* This phenomenon was not seen (at temperatures up to 550 K) in the other fcc interstitial alloy, Th-C (Fig. 5) [25].

saturation stress is plotted rather than the UTS.)

Figure 9 shows more particularly how strain hardening in this alloy depends on temperature [29]. In the dynamic strain-aging regime, there is a long plateau of constant strain-hardening rate (at a level of about half of the athermal hardening rate Θ_h typical of pure materials). It is almost independent of temperature in this range. Note, however, that eventually some dynamic recovery process does come in: the hardening rate decreases rather rapidly to zero (much before necking begins).

An interesting observation can be made on Fig. 9 that has some generality: the phenomenon of an extended linear hardening stage occurs even at 200 K, far below the dynamic strain-aging regime for this alloy. Similarly, Fig. 10 shows how the influence of P on strain hardening in Fe is pronounced (and similar) in both the region of jerky flow and at lower temperatures [30]. We are led to conclude either that phenomena akin to dynamic strain-aging occur far beyond the temperature range where jerky flow is observed[29,11] and exert their influence on dynamic recovery over this wider range; or that an influence of solutes on dynamic recovery is more general than by way of dynamic strain aging (or, most probably, both).

5. THE STACKING-FAULT ENERGY

A similar inhibiting effect of solute elements on dynamic recovery has been found in single crystals deforming in single slip, and has been interpreted as due to a lowering of the stacking-fault energy (SFE) [1]. The classical example of a strong change in SFE with concentration is Ni-Co. Results on single crystals of this alloy are shown in Fig. 11 [31], where the effect of solution hardening on easy glide (stage I work hardening) should be ignored for our purposes. It is evident that the stage II work-hardening rate

is not significantly affected by the additions of Co to Ni, but that the beginning of stage III is delayed -- the more so the higher the solute concentration.

It is possible that some of the observations reported in the last section, concerning an influence of solute additions on large-strain behavior, are also due to a lowering of the stacking-fault energy, although this does not seem likely, at least for Ni-C. Conversely, some contribution of strain-aging phenomena to the case of Ni-Co cannot be ruled out and is, in fact, probable in view of results on the strain-rate sensitivity [32].

6. MULTIPLICATIVE SOLUTION HARDENING

There are some sets of stress strain curves for solution hardened alloys that appear to diverge monotonically, right from the beginning. Figure 12 shows such a series for Al-Mg alloys at 78 K; the behavior is qualitatively similar at temperatures up to about 500 K [4]. Alloys of Cu-Zn [24,33,13], Cu-Al[34], and Al-Mg-Mn[35,36] exhibit similar behavior, as well as Fe-C, at least in some observations [37], and single crystals of Nb-W [38] and Nb-Mo [39]. In some cases, dynamic strain-aging is observed in the same regime, in many not; at least one may say that the phenomenon occurs over a much wider range of temperatures than jerky flow (as in Al-Mg, Fig. 12).

Figure 13 shows new results on Ni-Mo alloys[40]. It was found that a replot with a concentration dependent scale factor on the stress axis brings all of these curves into coincidence, so that these data (as well as similar curves taken T = 452 K) can be described empirically by the relation

$$\sigma = [1 + k(c)] \cdot \sigma_d \qquad (5)$$

This behavior is distinctly different from a divergence of the curves in the dynamic-recovery regime only. On the other hand, Fig. 14 demonstrates, for

the 3% alloy, that the dependence of strain hardening on temperature still follows the scheme outlined in Sec. 2: coincidence at small strains, divergence in the dynamic-recovery regime.

The difference between the effects discussed in the previous two sections and this one can be discussed with reference to eq. (3). While in the previous cases, we postulated a solute effect on a part ($\alpha\Theta_r$) of the net rate of dislocation storage $d\sqrt{\rho}/d\gamma$, it would seem that, in the present alloys, one of the other factors must be responsible that are constant throughout the strain range. The dependence of the shear modulus and the lattice constant on concentration are much too weak for the magnitude of k observed. The only remaining possibility for the principal cause of the strengthening is α. It reflects the strength of dislocation/forest interactions. Schmidt and Miller [7] have recently made a similar proposal.

7. A UNIFYING MECHANISM

The empirical equation (5) has some similarity to relations observed recently in static and dynamic strain-aging experiments. We shall first summarize these results, and then relate them to effects outside the dynamic-strain-aging regime and, in fact, outside the regime of solute bulk-mobility. A simple mechanism will then be qualitatively outlined that may underlie all these phenomena.

7.1 Strain Aging

The term "strain" aging relates to the appearance, upon aging at (or above) the current deformation temperature, of a yield point that depends in its magnitude on the strain level achieved before aging. It has recently been postulated, and in some cases experimentally verified over a significant regime, that the yield drop $\Delta\sigma_a$ is linearly related to the stress reached in

the previous straining [8,9]; viz., essentially proportional to σ_d:

$$\Delta\sigma_a = k'(c)\cdot\sigma_d \qquad (6)$$

Equation (6) has the same form as the concentration dependent stress increment in eq. (5).

7.2 Dynamic Strain-aging

Dynamic strain-aging is currently considered to be due to the same process as static strain-aging, occurring during the normal waiting time of dislocations in their generally jerky progress through the slip plane [42,29,41]. Since this waiting time is inversely proportional to the imposed strain rate, the aging process makes a negative contribution to the strain-rate sensitivity of the flow stress: slower strain rates allow more aging and therefore more hardening.

It was found by Mulford [29,32] that this negative contribution to the strain-rate sensitivity is again proportional to σ_d, at least in some Ni alloys and Al-Mg, at not too high strains:

$$\Delta\frac{\partial\sigma}{\partial\ln\dot{\varepsilon}}\Big|_T = -k''(c)\cdot\sigma_d \qquad (7)$$

This is in agreement with the observation, on the same alloys [8,9], of static aging according to eq. (6). The critical strain for the beginning of jerky flow is then interpreted as that at which the total strain-rate sensitivity becomes negative [12,41]. Note, however, that a negative contribution to the rate sensitivity, which is evidence of dynamic strain-aging, may not be sufficient to offset other, positive contributions; then, jerky flow does not occur. The Ni-Mo alloys quoted above are a case in point, and so is Ni-Co[32] -- and in both these cases, the initial negative contribution is proportional to σ_d.

We conclude that the proportionality to the flow stress, which is observed for the stress increments in strain-hardening (eq. 5), static strain-

aging (eq. 6), and dynamic strain-aging (eq. 7), may be a common feature associated with solute mobility, whether or not this causes jerky flow. It can be observed at lower temperatures than jerky flow.

7.3 The Low-temperature Yield Strength

There have long been difficulties with explanations of the yield strength based on the concept of solute atoms acting as discrete obstacles [43,44]. Principally, the observed rate and temperature dependence are much too low for this mechanism to hold [45]. In terms of dislocation activation, the activation length inferred from measurements of the apparent activation area [42] is large compared to the solute spacing along the dislocation [45] and, most importantly, is not proportional to it [11]. These problems are pronounced in the regime of the "plateau" in the yield stress vs temperature diagram (which often occurs at quite moderate temperatures), but were also shown to be substantial at lower temperatures.

On the other hand, a description of solution hardening in terms of the formulas proposed by Suzuki [10] is much more successful. The essence of the underlying mechanism (whether or not the details of this particular theory apply) is that the solutes behave as if they were continuously, not discretely, distributed along the dislocation. In combination with an assumption of some ability of the solutes to redistribute themselves within the dislocation core (perpendicular to the dislocation [46]), this leads to a model in which the dislocation "digs its own trough" while waiting at "hard lines" and must continuously free itself from each new trough [11].

Thermal activation from such a trough occurs by the formation of a bulge in the dislocation line (Fig. 15), whose length ℓ_b is inversely proportional to the stress [42] (or, more exactly, the stress in excess of σ_d). This length is generally much larger than the solute spacing, and gets larger as

the temperature is raised. This can give an almost plateau-like effect: the unlocking stress becomes inversely proportional to temperature at high temperatures — unless another effect intervenes.

7.4 The High-temperature Limit of the Unlocking Stress

If the activation length in unlocking gets longer and longer as the temperature is raised, there eventually comes a point when the length of the bulge would begin to exceed the forest-dislocation spacing ℓ_d. This cannot happen, and it is at this point that the unlocking stress becomes proportional to σ_d: the strength of the forest junction is augmented by the force to form the bulge. Instead of eqs. (2) and (3), we then have

$$\sigma = [\alpha(T,\dot{\varepsilon}) + \beta(c,T,\dot{\varepsilon})] \cdot M \mu b \sqrt{\rho} = \sigma_d \cdot (1 + \beta/\alpha) \qquad (8)$$

Note that the term proportional to β has taken the place of σ_f: no further additive friction stress is needed.

The quantity β in eq. (8) is the angle at which the activation bulge meets the dislocation (Fig. 15). It can be derived when the profile of the line-tension trough is known, and depends on temperature and strain rate [42].

Equation (8) could form the basis of a unified description of all the phenomena discussed above: it is formally similar, and the mechanism of repeated locking and unlocking seems especially attractive in the elevated-temperature regime. Much quantitative work needs to be done to ascertain the viability of this proposal.

8. CONCLUSIONS

We have discussed three distinct effects of solute additions to the flow stress, and their relation to the flow stress contribution from strain hardening, σ_d: an additive friction stress (σ_f); a multiplicative "repeated-unlocking" stress (interpreted as an additive effect on the dislocation/

dislocation interaction strength α); and a decrease in the rate of dynamic recovery (θ_r). We find that the first, which is the most discussed, may be strictly absent in the high-temperature limit, but is certainly negligible at all but the smallest of strains. On the other hand, the second, a multiplicative solution strengthening, which is the least discussed, is probably the most general contribution over the widest range of elevated temperatures. In the dynamic strain-aging regime, the effect on dynamic recovery becomes dominant.

While the effects were here discussed for cases where one or the other of them predominates, they will, in most cases, act in concert. For example, a re-examination of the figures presented in the section on dynamic strain-aging and dynamic recovery will show some evidence of the proportional effect acting also. However, when this is taken into account, a significant additional effect on dynamic recovery remains.

In general (but neglecting σ_f), the flow stress of solution hardened alloys may then be written, instead of as eq. (2), as

$$\sigma = \mu(T,c)\cdot\alpha_c(c,T,\dot{\varepsilon})\cdot\int\frac{\theta}{\mu\alpha_c}\,d\varepsilon \qquad (9)$$

where α_c is used for $[\alpha+\beta]$ in eq. (8). The integrand represents the (net) rate of dislocation storage (eq. 4), and may be expressed, by way of generalizing eq. (1), as

$$\frac{\theta}{\mu\alpha_c} = \frac{\theta_h}{\mu\alpha_c} - \frac{\theta_r}{\mu\alpha_c}\left(\frac{\sigma}{\mu\alpha_c},T,\dot{\varepsilon},c\right) \qquad (10)$$

We cannot envisage any possible influence of solutes on the first term on the right-hand side, which represents statistical dislocation storage.* The effect on the rate of dynamic recovery may be due in part to a decrease in the

---

* Note that Schmidt and Miller [7] combine what we would call "dynamic recovery" with hardening (which they assume parabolic in strain) and separate out "recovery" (occurring simultaneously with straining); they expect solutes to influence both of their terms.

stacking-fault energy, but is most significantly influenced by dynamic strain-aging. Thus, it is particularly important in an intermediate, elevated temperature regime.

The flow stress in the steady-state limit follows from setting the right-hand side of eq.(10) to zero. The result is of the form

$$\sigma_s = \mu(T,c)\cdot\alpha_c(c,T,\dot{\varepsilon})\cdot F(T,\dot{\varepsilon},c) \qquad (11)$$

It looks very much like eq.(9), except that the strain-dependent integral has been replaced by a constant F, depending only on T, $\dot{\varepsilon}$, and c. The latter effect is, again, due to the influence of solutes on dynamic recovery and is potentially the most important, at elevated temperatures. It is not possible, in principle, to separate the effects on α_c and F when only deformation at (or near) steady state is studied.

To distinguish flow stress effects from evolution effects of solute additions, one must study the strain-hardening behavior. First, one analyze stress strain curves according to eqs. (9) and (10), manipulating α_c in eq. (10) to produce coincidence for different concentrations at small strains and low temperatures; any remaining difference to be interpreted as due to Θ_r. Second, one may undertake microscopic structure investigations on alloys of different concentrations : over the strain range in which no Θ_r-effect is detected, the relevant substructural features should be independent of concentration at the same strain, even though the stresses themselves may be significantly different. Finally, one should vary the thermomechanical history : effects on α_c depend only on the current values of the external and structural variables, whereas the integral depends on the entire strain path [7].

The multiplicative flow stress effect is new, having been discussed only once, in somewhat different form, by Schmidt and Miller [7]. An explanation is offered that relates it to other solute effects currently under discussion.

The model is based on the concept that "moving" dislocations must continually free themselves from continuous line-tension troughs (rather than from discrete solute atoms). These troughs get deeper as solutes diffuse to the momentarily waiting dislocation (but they exist even at very low temperatures [11]). The stacking-fault ribbon may play a role in the establishment of an effective "trough"[10]. The process of unlocking occurs by the formation of a bulge whose length is inversely proportional to the stress. At low stresses, i.e. high temperatures, the bulge length equals the forest dislocation spacing, which it cannot exceed. From this point on, the solute/dislocation interaction has the effect of merely raising the effective strength of the dislocation/dislocation interaction. For this reason, all solute effects are now proportional, as the dislocation density increases, to the strain-hardening contribution to the flow stress, σ_d: the static strain-aging stress peak; the decrease in the strain-rate sensitivity; and the flow stress increment itself.

The proposed mechanism is as yet of a rather qualitative nature; it suggests a number of experiments to quantitatively ascertain the various correlations.

Acknowledgments — It is a pleasure to acknowledge the contribution made by my coworkers T. A. Bloom and R. E. Cook to the unpublished work on Ni-Mo and Ni-C alloys, as well as their valuable comments on the manuscript. This work was supported by the U. S. Department of Energy.

REFERENCES

1. P. Haasen, in Fundamental Aspects of Structural Alloy Design, R. I. Jaffee and B. A. Wilcox, eds. (Plenum 1977), p. 3.
2. W. C. Leslie, Met. Trans. 3, 5 (1972).
3. U. F. Kocks, in Strength of Metals and Alloys, P. Haasen, V. Gerold, and G. Kostorz, eds. (Pergamon, 1980) p. 1661.
4. O. D. Sherby, R. A. Anderson, and J. E. Dorn, J. Metals 3, 643 (1951).
5. J. D. Embury, in Strengthening Methods in Crystals, A. Kelly and R. B. Nicholson, eds. (Elsevier 1971), p. 331.
6. H. Chandra-Holm and J. D. Embury, to be published.
7. C. G. Schmidt and A. K. Miller, Acta Metall. 30, 615 (1982).
8. P. Wycliffe, U. F. Kocks, and J. D. Embury, Scripta Met. 14, 1349 (1980).
9. U. F. Kocks and R. E. Cook, to be published.
10. H. Suzuki, in Dislocations and Mechanical Propertiues of Crystals, J. C. Fisher et al., eds.(Wiley 1957) p. 361; and in Strength of Metals and Alloys, P. Haasen, V. Gerold, and G. Kostorz, eds.(Pergamon 1979) p. 1595.
11. U. F. Kocks, to be published.
12. U. F. Kocks, Prog. Mater. Sci., Chalmers Anniv. Vol., 185 (1981).
13. J. Gil Sevillano, P. van Houtte, E. Aernoudt, Prog. Mater. Sci. ??, p.90.
14. S. S. Hecker, M. G. Stout, and D. T. Eash, in Proc. Plasticity of Metals at Finite Strain, E. Lee, ed. (Stanford University 1981).
15. U. F. Kocks, H. S. Chen, D. A. Rigney, R. J. Schaefer, in Work Hardening, J. P. Hirth and J. Weertman, eds. (Gordon and Breach 1968), p. 151.
16. H. Mecking, in Work Hardening in Tension and Fatigue, A. W. Thompson, ed. (AIME, 1977) p. 67.
17. U. F. Kocks, J. Eng. Mater. Tech. (ASME series H) 98, 76 (1976).
18. H. Mecking and U. F. Kocks, Acta Metall. 29, 1865 (1981).

19. J. Diehl, Z. Metallk. 47, 331 (1956).

20. E. Voce, J. Inst. Metals 74, 537 (1948).

21. B. Nicklas and H. Mecking, in Strength of Metals and Alloys, P. Haasen, V. Gerold, and G. Kostorz, eds. (Pergamon, 1979) p. 351.

22. H. Mecking and A. Grinberg, in Strength of Metals and Alloys, P. Haasen, V. Gerold, and G. Kostorz, eds. (Pergamon, 1979) p. 289.

23. M. M. Hutchison and R. W. K. Honeycombe, Metal Sci. J. 1, 70 (1967).

24. G. J. den Otter and A. van den Beukel, phys.stat.sol.(a)55, 785 (1979).

25. D. T. Peterson and R. L. Skaggs, Trans. AIME 242, 922 (1968).

26. J. D. Baird and C. R. MacKenzie, J. Iron Steel Inst. 202, 427 (1964).

27. C. F. Jenkins and G. V. Smith, Trans. AIME 245, 2149 (1969).

28. Y. N. Dastur and W. C. Leslie, Met. Trans. 12A, 749 (1981).

29. R. A. Mulford and U. F. Kocks, Acta Metall. 27, 1125 (1979).

30. W. A. Spitzig, Mater. Sci. Eng. 16, 169 (1974).

31. J. Meissner, Z. Metallk. 50, 207 (1959).

32. R. A. Mulford, Acta Metall. 27, 1115 (1979).

33. A. Korbel, L. Błaz, H. Dybiec, J. Gryziecki, and J. Zasadziński, Metals Technology 1979, p. 391.

34. L. Gastberger, O. Vöhringer, E. Macherauch, Z. Metallk. 65, 17 (1974).

35. J. G. Morris, Mater. Sci. Eng. 13, 101 (1974).

36. H. Herø, Proc. 10th Biennial Congr. Intern. Deep Drawing Res. Group (Warwick 1979), p. 179.

37. D. J. Quesnel, A. Sato, and M. Meshii, Mater. Sci. Eng. 18, 199 (1975).

38. G. Kostorz, Z. Metallk. 59, 941 (1968).

39. P. Jax, Z. Metallk. 62, 284 (1971).

40. T. A. Bloom, U. F. Kocks, and P. Nash, to be published.

41. A. van den Beukel and U. F. Kocks, Acta Metall. 30, 1027 (1982).

42. U. F. Kocks, A. S. Argon, and M. F. Ashby, Prog. Mater. Sci. 19, 1 (1975).

43. R. L. Fleischer, in The Strengthening of Metals (Reinhold, 1964) p. 93.

44. R. Labusch, Acta Metall. 20, 917 (1972).

45. Z. S. Basinski, R. A. Foxall, and R. Pascual, Scripta Met. 6, 807 (1972).

46. R. B. Schwarz and L. L. Funk, Acta Metall.

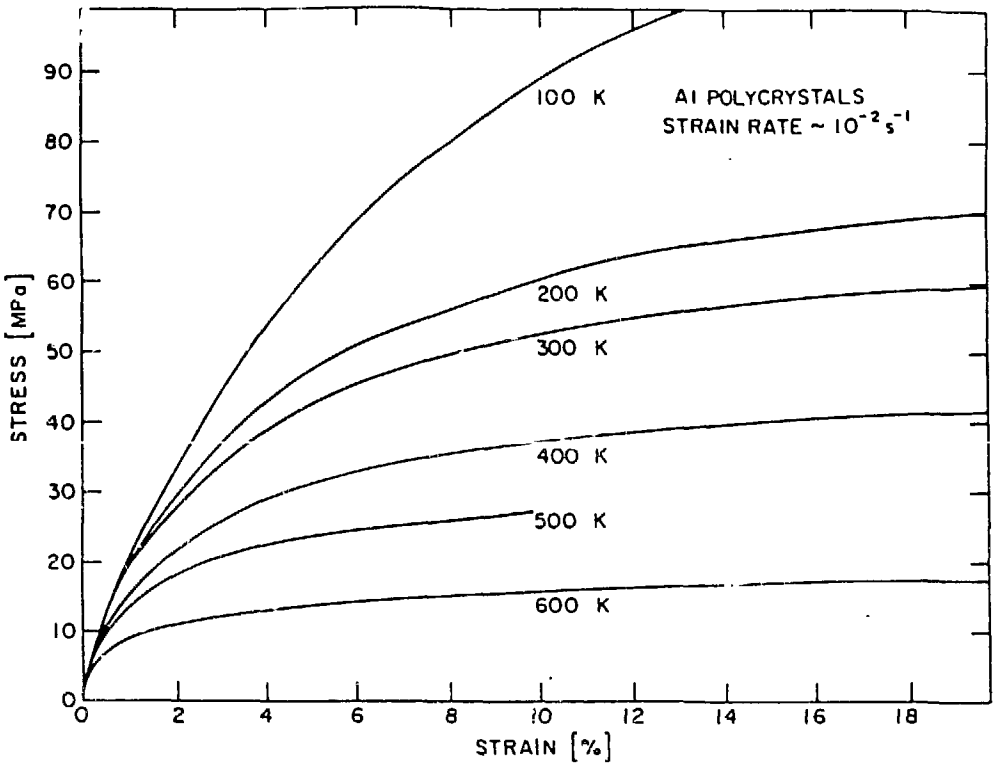

Fig. 1. Nominal tensile stress strain curves for aluminum (99.99%, grain size d = 0.2 mm). After Kocks et al. [15].

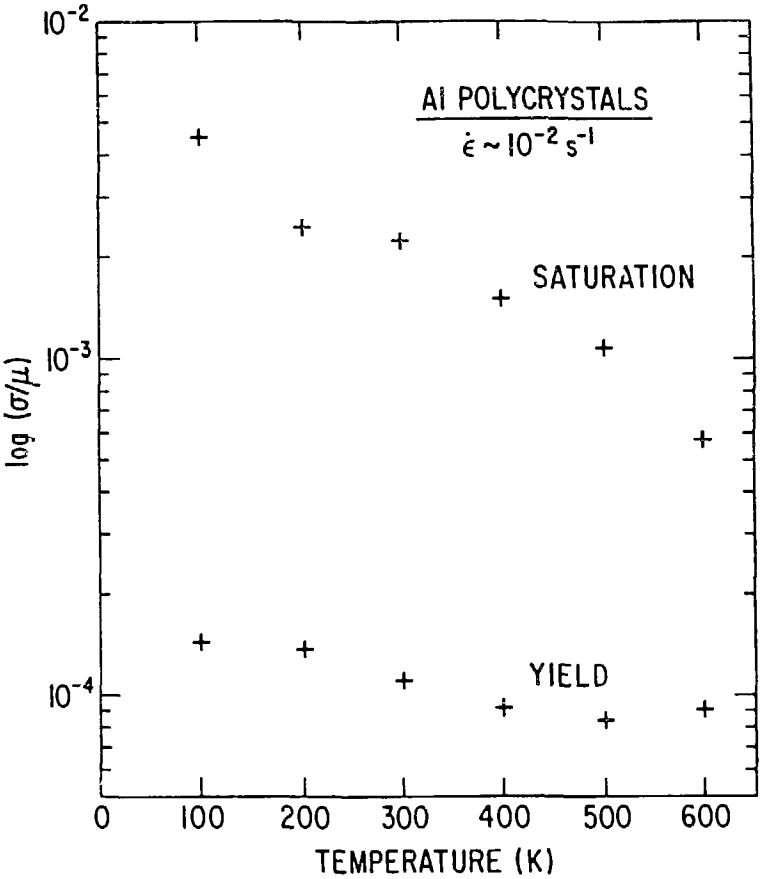

Fig. 2. Yield stress and true saturation stress, divided by shear modulus, as a function of temperature. Data from Fig. 1.

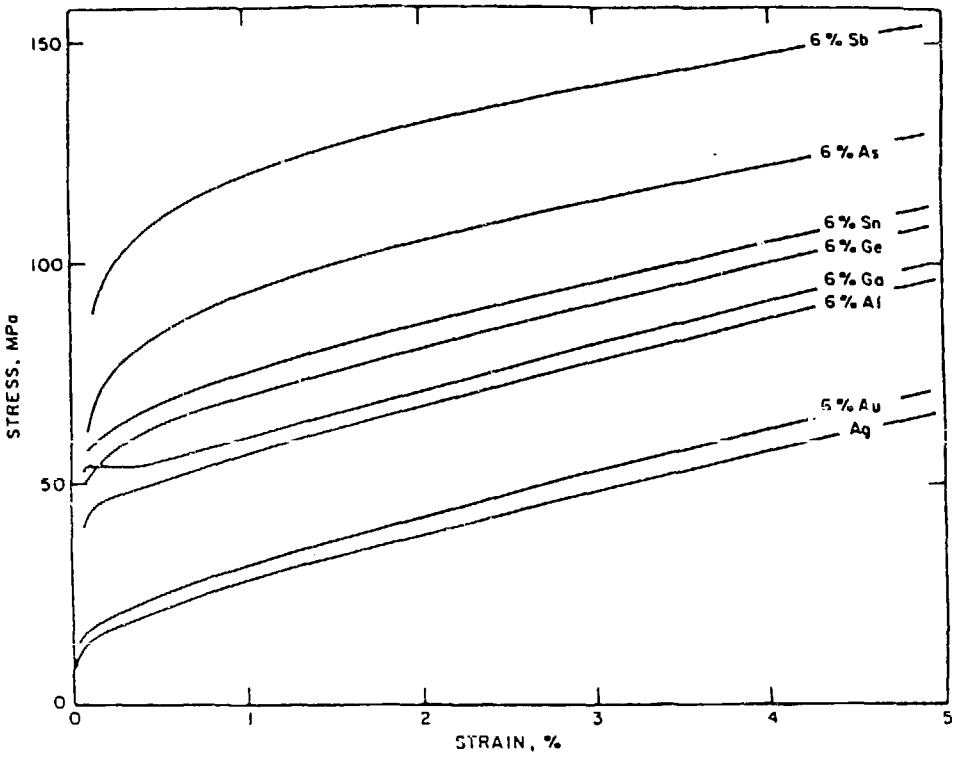

Fig. 3. True tensile stress strain curves for silver alloys (d ≈ 50 μm), tested at 77 K. After Hutchinson and Honeycombe [23].

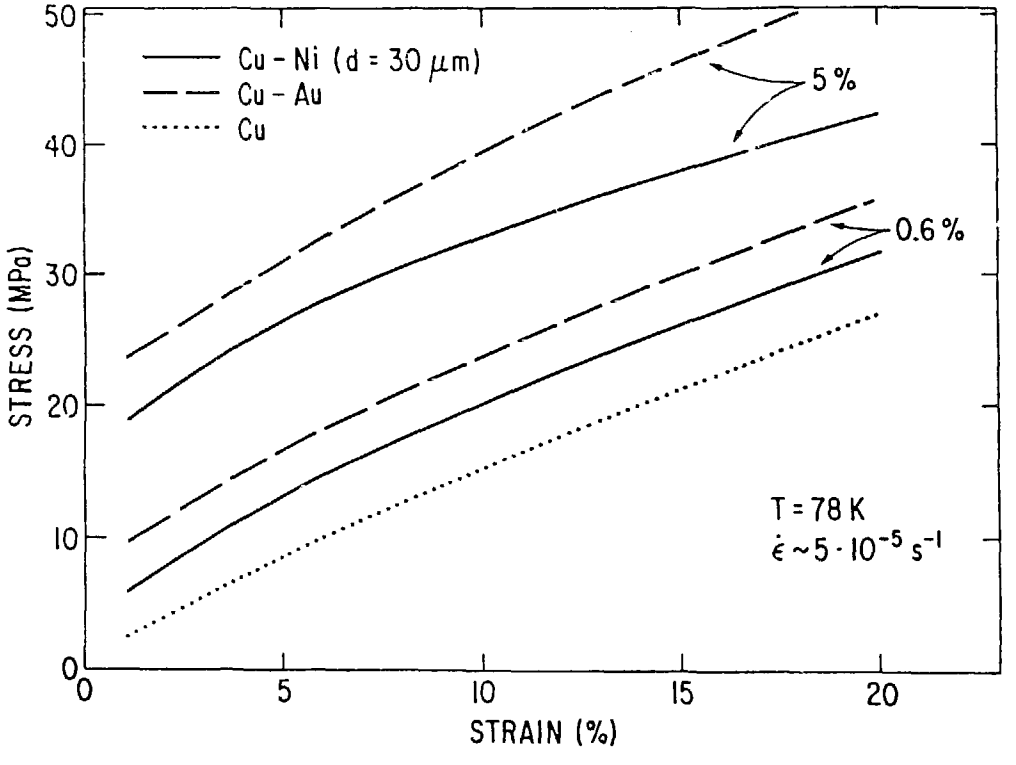

Fig. 4. Tensile stress strain curves for copper-nickel and copper-gold alloys of two concentrations. After den Otter and van den Beukel [24].

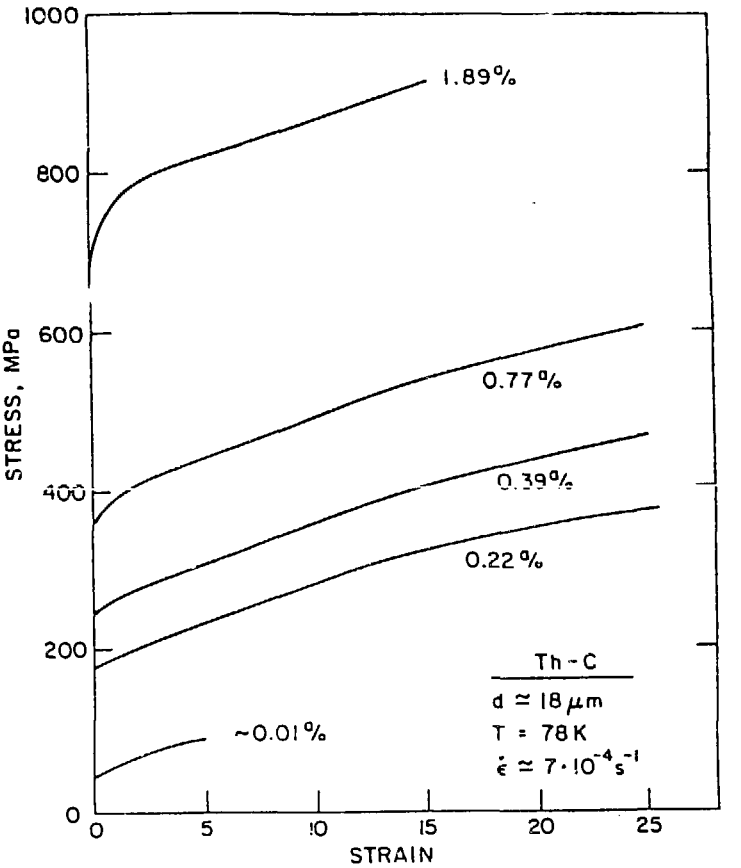

Fig. 5. True tensile stress strain curves for thorium-carbon alloys. After Peterson and Skaggs [25].

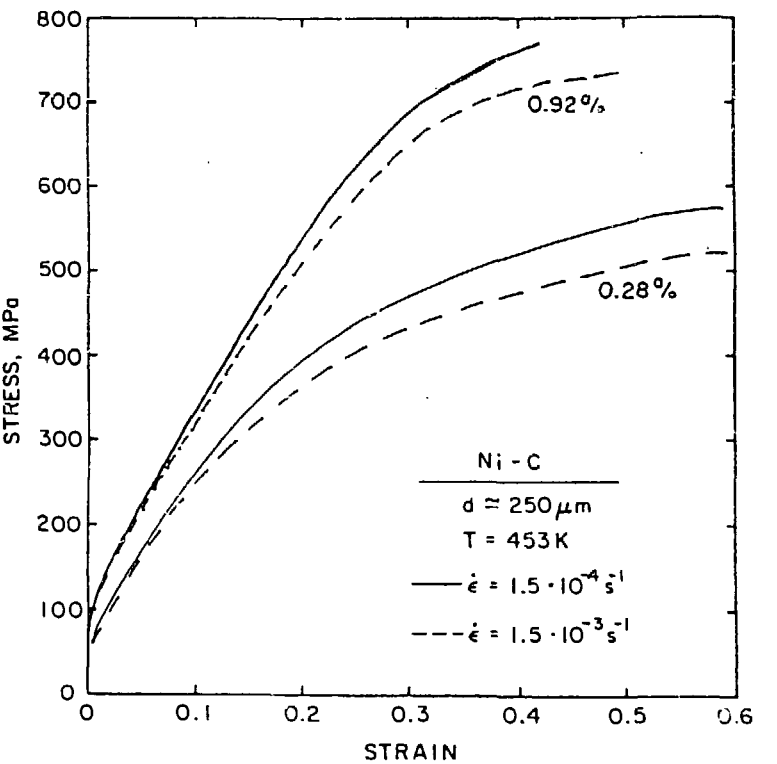

Fig. 6. True compressive stress strain curves for two nickel-carbon alloys. The higher strain rate (dashed) produces the lower strain hardening, indicating an influence of dynamic strain-aging on dynamic recovery. New results [9].

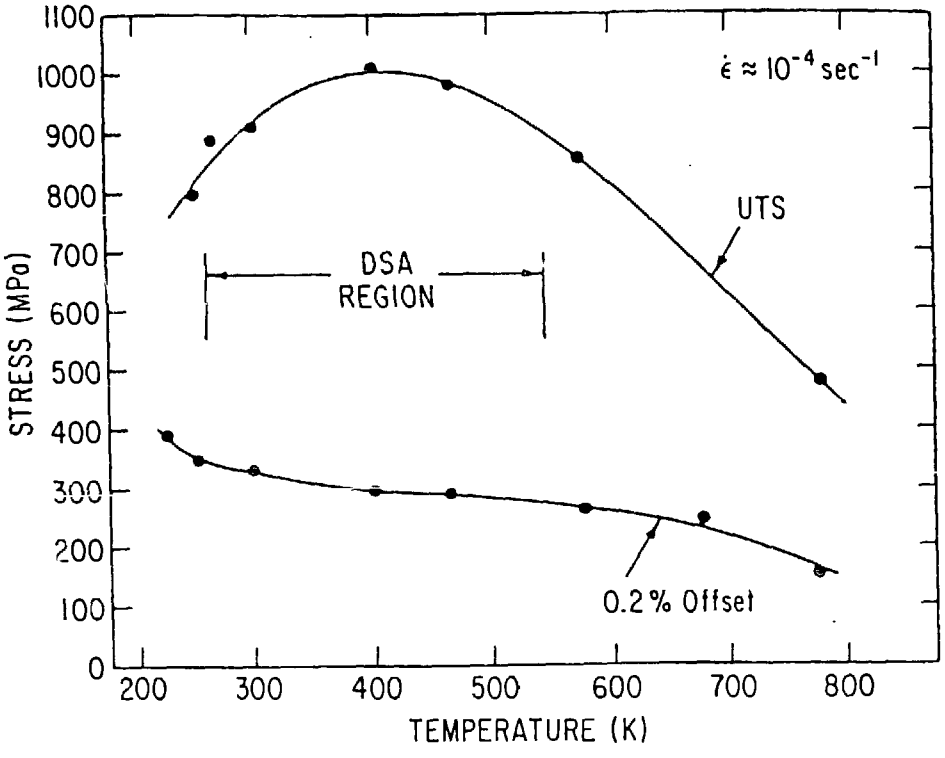

Fig. 7. Yield stress and tensile strength as a function of temperature for Hadfield steel, showing the pronounced influence of dynamic strain aging on the UTS. After Dastur and Leslie [28].

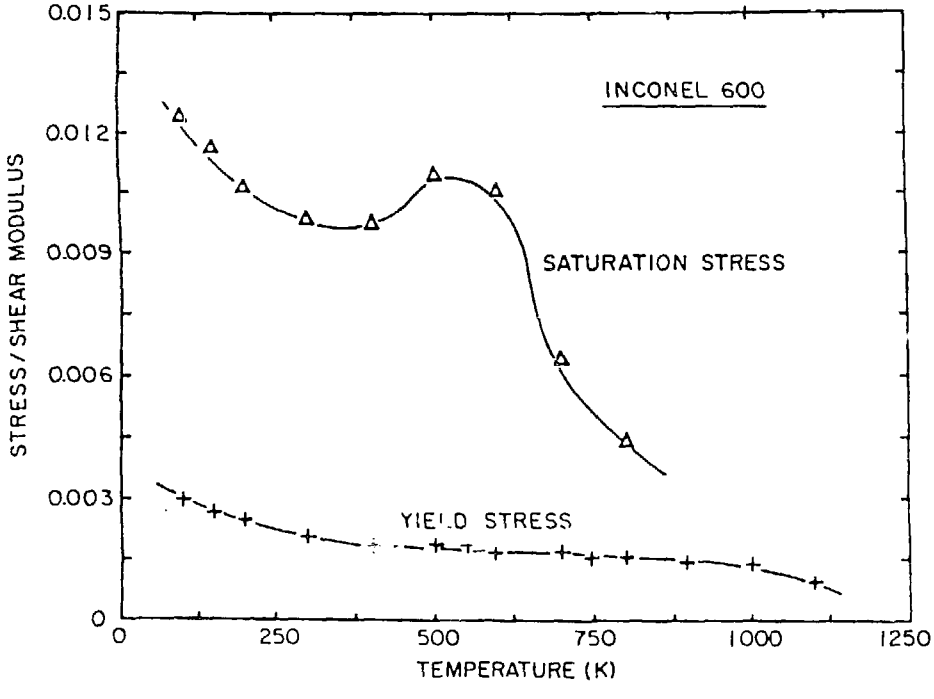

Fig. 8. Yield stress and saturation stress, divided by shear modulus, as a function of temperature, for INCONEL 600. From Mulford and Kocks [29].

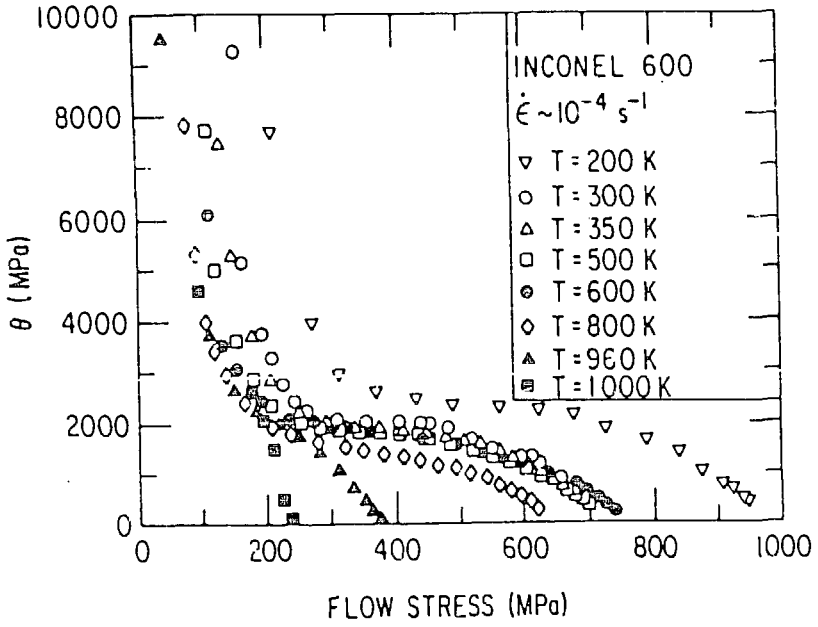

Fig. 9. Strain hardening rate $\Theta = d\sigma/d\varepsilon$ as a function of flow stress for INCONEL 600. Note the temperature-insensitive plateau between 300 and 600 K. From Mulford and Kocks [29].

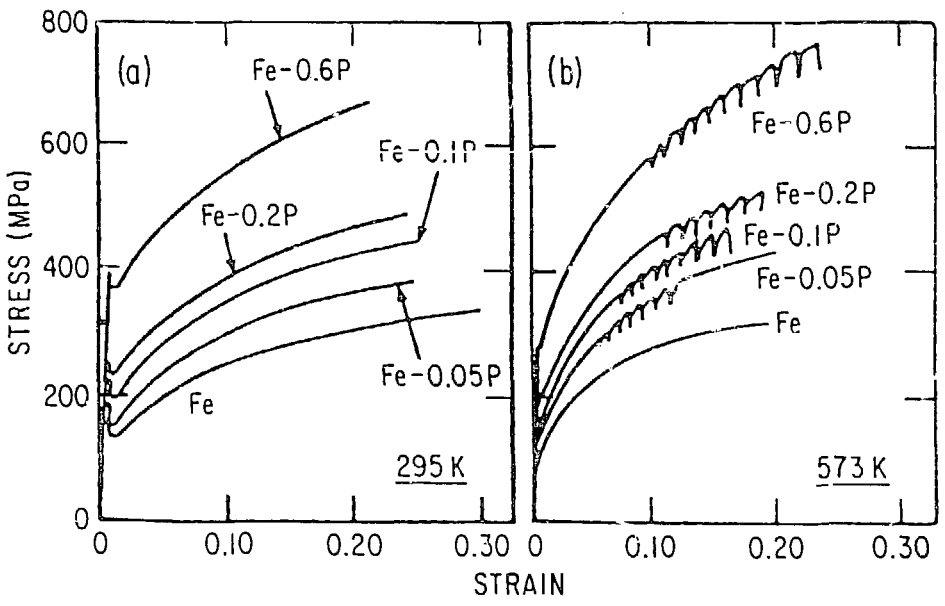

Fig. 10. True tensile stress strain curves for iron-phosphorus alloys tested (a) below and (b) within the jerky-flow regime. The approximate P-content is given in wt.%. After Spitzig [30].

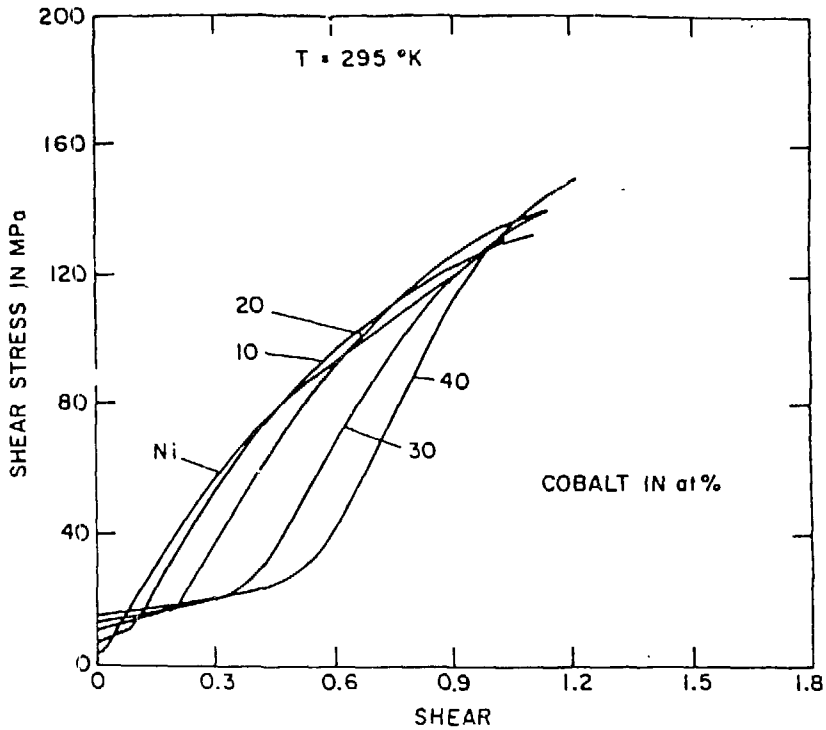

Fig. 11. Resolved shear stress vs shear curves for nickel-cobalt single crystals of a central orientation. Note the continual decrease of dynamic recovery with increasing concentration. After Meissner [31].

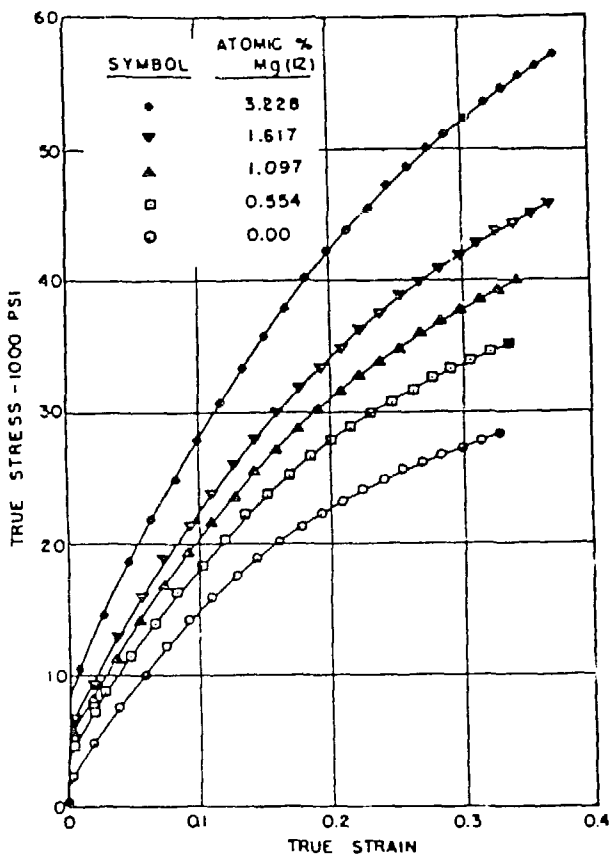

Fig. 12. True tensile stress strain curves for aluminum-magnesium alloys (d = 0.3 mm), tested at 78 K at a strain rate of $2 \cdot 10^{-3} s^{-1}$. After Sherby, Anderson and Dorn [4].

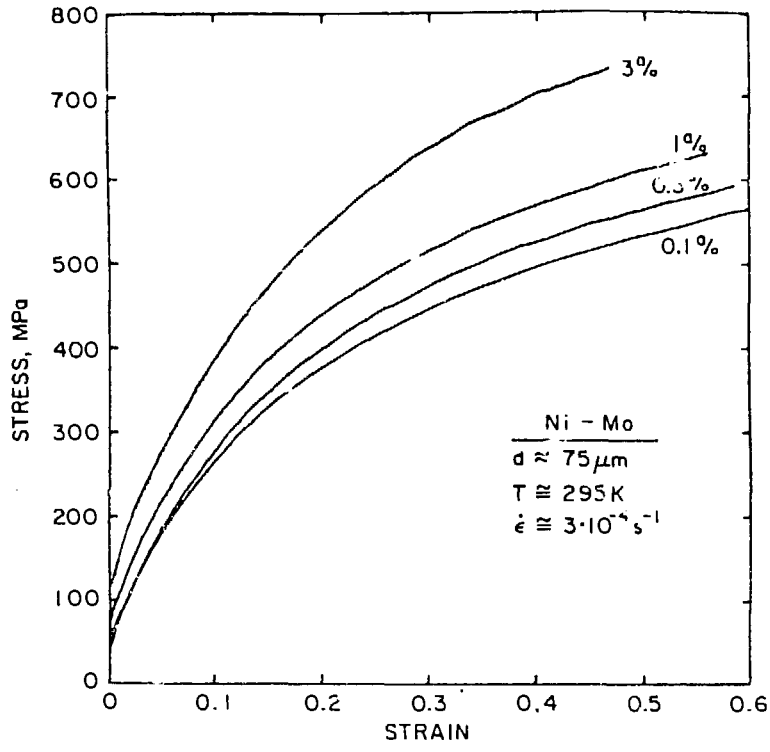

Fig. 13. True compressive stress strain curves for nickel-molybdenum alloys. They diverge monotonically. New results [40].

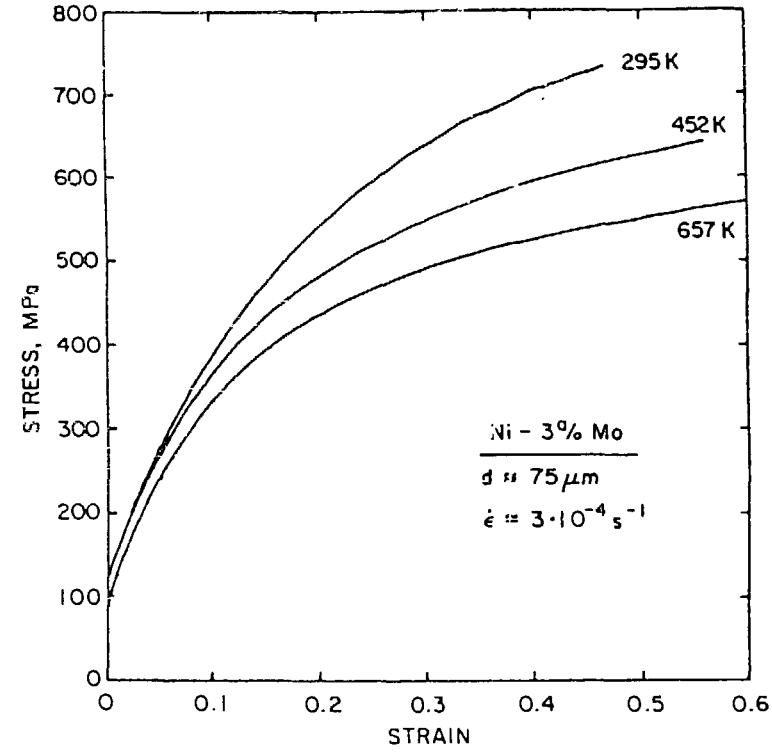

Fig. 14. True compressive stress strain curves for one Ni-Mo alloy at three temperatures. They coincide at low strains, but diverge in the dynamic-recovery regime. New results [40].

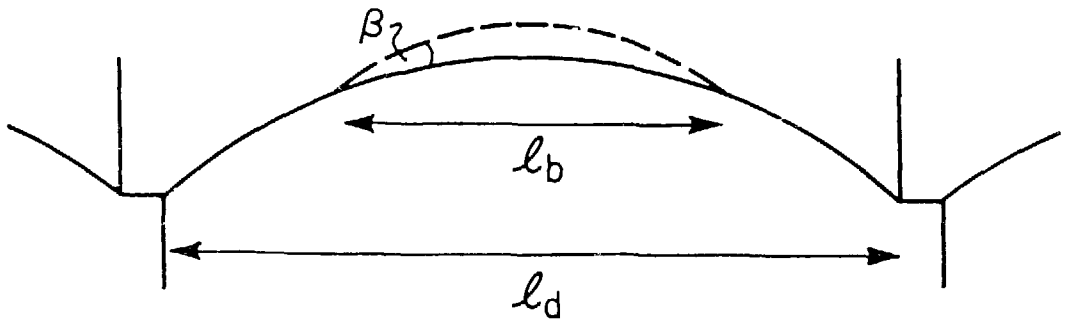

Fig. 15. Locked dislocation segment with activated bulge (dashed). Its curvature is determined by the stress, the angle β by the line tension difference.